Coronal mass ejection–driven shocks and the associated sudden commencements/sudden impulses

B. Veenadhari,[1,2] R. Selvakumaran,[1] Rajesh Singh,[3] Ajeet K. Maurya,[1] N. Gopalswamy,[4] Sushil Kumar,[5] and T. Kikuchi[2]

Received 30 September 2011; revised 8 February 2012; accepted 12 February 2012; published 11 April 2012.

[1] Interplanetary (IP) shocks are mainly responsible for the sudden compression of the magnetosphere, causing storm sudden commencement (SC) and sudden impulses (SIs) which are detected by ground-based magnetometers. On the basis of the list of 222 IP shocks compiled by Gopalswamy et al. (2010), we have investigated the dependence of SC/SIs amplitudes on the speed of the coronal mass ejections (CMEs) that drive the shocks near the Sun as well as in the interplanetary medium. We find that about 91% of the IP shocks were associated with SC/SIs. The average speed of the SC/SI-associated CMEs is 1015 km/s, which is almost a factor of 2 higher than the general CME speed. When the shocks were grouped according to their ability to produce type II radio burst in the interplanetary medium, we find that the radio-loud (RL) shocks produce a much larger SC/SI amplitude (average ∼32 nT) compared to the radio-quiet (RQ) shocks (average ∼19 nT). Clearly, RL shocks are more effective in producing SC/SIs than the RQ shocks. We also divided the IP shocks according to the type of IP counterpart of interplanetary CMEs (ICMEs): magnetic clouds (MCs) and nonmagnetic clouds. We find that the MC-associated shock speeds are better correlated with SC/SI amplitudes than those associated with non-MC ejecta. The SC/SI amplitudes are also higher for MCs than ejecta. Our results show that RL and RQ type of shocks are important parameters in producing the SC/SI amplitude.

Citation: Veenadhari, B., R. Selvakumaran, R. Singh, A. K. Maurya, N. Gopalswamy, S. Kumar, and T. Kikuchi (2012), Coronal mass ejection–driven shocks and the associated sudden commencements/sudden impulses, *J. Geophys. Res.*, *117*, A04210, doi:10.1029/2011JA017216.

1. Introduction

[2] Interplanetary (IP) shocks driven by coronal mass ejections (CMEs) originating close to the solar disk center often arrive at Earth and compress the magnetosphere causing the storm sudden commencement (SC). A SC is an increase in the horizontal component of Earth's magnetic field measured by ground-based magnetometers at the low latitudes and is often followed by a geomagnetic storm if the interplanetary CME (ICME) driving the shock and/or the shock sheath contains southward pointing magnetic field [*Tsurutani et al.*, 1988; *Gonzalez et al.*, 1994; *Gopalswamy*, 2008]. In addition to IP shocks, sudden increases in the solar wind dynamic pressure can also affect the magnetosphere causing sudden impulses (SI) which are identified with sudden increase in magnetic field at geosynchronous orbit and also at the ground by magnetometers [*Araki*, 1977; *Takeuchi et al.*, 2002; *Wilken et al.*, 1982; *Chi et al.*, 2006]. SC/SIs can be clearly seen as an increase in the ground-based magnetic field intensity which typically lasts for tens of minutes and then followed by a geomagnetic storm. The term SC is used when it occurs at the beginning of the initial phase of a magnetic storm, whereas SI is a general term including occurrences outside the storm interval.

[3] There have been a number of studies that have shown that most (80%–90%) of the SC/SIs are associated with IP shocks and only a small number are caused by tangential discontinuities [*Chao and Lepping*, 1974; *Smith et al.*, 1986]. *Wang et al.* [2006] surveyed IP shocks and SCs observed from 1995 to 2004 and found that about 75% of SCs are associated with IP shocks. They also reported that the SC risetime is dependent on IP shock speed. IP shock orientation also plays an important role in determining the SC risetime as a highly oblique shock requires more time to compress the forward part of magnetosphere [*Wang et al.*, 2006].

[4] *Wang et al.* [2009] performed a statistical survey of the relation between geosynchronous magnetic field changes

[1]Department of Science and Technology, Indian Institute of Geomagnetism, Navi Mumbai, India.
[2]Solar-Terrestrial Environment Laboratory, Nagoya University, Nagoya, Japan.
[3]Dr. K. S. Krishnan Geophysical Research Laboratory, Indian Institute of Geomagnetism, Jhunsi, India.
[4]NASA Goddard Space Flight Center, Greenbelt, Maryland, USA.
[5]School of Engineering and Physics, University of the South Pacific, Suva, Fiji.

0148-0227/12/2011JA017216

and sudden impulses due to IP shocks observed from 1998 to 2005. They found that 216 of the 250 IP shocks (~88%) produced changes in the geosynchronous magnetic field observed by GOES satellites and SIs as detected by the change in the *SYM-H* index and 75% negative responses (negative sudden impulses) in the midnight sector were associated with southward interplanetary magnetic field. Recently, *Wang et al.* [2010] suggested that SIs can be used to estimate some of the interplanetary parameters at the L1 point and at geosynchronous orbit, including the changes in solar wind dynamic pressure across the shock and the associated geosynchronous magnetic field changes near the subsolar region.

[5] The above mentioned studies are confined to IP shocks observed in the solar wind near Earth. But IP shocks undergo considerable changes as they propagate from near the Sun to the L1 point. The best way to characterize them is to examine the CMEs that drive them. CMEs can be observed by coronagraphs very close to the Sun (one to 2 solar radii above the surface). Such early observations can provide advance warning of shocks arriving at Earth by more than half a day to a few days. Shocks near the Sun are inferred from type II radio bursts in the solar corona and IP medium. Every large solar energetic particle (SEP) event is associated with a type II radio burst which is used as a strong evidence for particle acceleration by shocks. When shocks arrive at Earth, they can be identified from the energetic storm particle (ESP) events. The energetic electrons are unstable to Langmuir waves, which get converted into radio emission at the local plasma frequency and its harmonics. This radio emission is said to be type II radio burst. The shocks which produce the type II radio burst are said to be radio loud (RL) and those which do not produce type II burst are said to be radio quiet (RQ) [*Gopalswamy et al.*, 2010]. The CMEs associated with RL shocks are said to be RL CMEs and those followed by the IP shocks are said to be RL IP shocks, or simply RL shocks. Similarly, there are RQ CMEs and RQ IP shocks (or simply RQ shocks). Electrons accelerated in CME-driven shocks generate type II radio bursts observed in dynamic radio spectra as intermittent or continuous sweeps that slowly decrease in the frequency. Recently, *Cho et al.* [2010] considered 26 RL CMEs and the resulting IP shocks. They found that the CME speed is highly correlated with SC amplitude and concluded that only fast CMEs (speed greater than 1600 km/s) could cause the magnetopause crossing of geosynchronous orbit. *Cho et al.* [2010] investigation considered only ~10% of all IP shocks and confined only to a small number of RL CMEs. Of course, not all IP shocks are associated with type II radio bursts, but one can still identify the driving CMEs from coronagraphic observations. Such radio-quiet (RQ) shocks constitute a large fraction (~34%) of all IP shocks [*Gopalswamy et al.*, 2010, hereinafter referred to as paper 1]. Therefore, it is very important to consider both the RL and RQ CMEs that result in IP shocks and the resulting dynamic pressure increases at L1 as well as the SCs. The RL CMEs considered by *Cho et al.* [2010] were based on metric type II bursts alone, but it is well known that type II bursts occur at all wavelengths from metric to kilometric domain corresponding to the corona and IP medium [*Gopalswamy et al.*, 2005]. Thus, we consider all CME-driven shocks from those that do not produce type II radio emission to those that produce radio emission at all wavelengths.

[6] When shock-driving CMEs arrive at Earth, they can be observed as a magnetic cloud (MC) or noncloud ejecta (EJ). It is also important to consider the ICME type (MC or EJ) because they seem to represent head-on and glancing blows to the magnetosphere [*Gopalswamy*, 2009] and hence may have implications to the resulting SCs. The CME and radio emission characteristics are useful in understanding the shock-driving ability of CMEs near the Sun because type II bursts are the earliest indicators of shocks and contain information on both the shock and the ambient medium in which shock propagates [*Gopalswamy et al.*, 2008a, 2008b]. The new findings reveal that some of the shocks are not associated with type II bursts near the Sun or in the IP medium (paper 1). It is of interest to know how the CMEs with and without the associated radio bursts affect the magnetosphere, as indicated by SC/SI.

[7] Paper 1 used a larger data set of 222 IP shocks detected by spacecraft at the Sun–Earth L1 during solar cycle 23 (1996 to 2006, inclusive) to carry out an extensive study of RL and RQ IP shocks. This work found that the distinction between RL and RQ shocks is relatively small even though the difference in the properties of driving CMEs was significantly large. We make use of the extensive database on IP shocks, ICMEs, CMEs, and type II radio bursts (paper 1) in our attempt to understand the characteristics of SCs. The list of IP shocks compiled in paper 1 forms the basis for the present study details of which are briefly given in section 2.

2. Data

[8] The 222 IP shocks listed in paper 1 were observed at 1 AU by one or more of the three spacecraft: the Advanced Composition Explore (ACE), the Solar and Heliosphere Observatory (SOHO), and the Wind spacecraft during solar cycle 23 (1996–2006, inclusive). Table 1 in paper 1 gives the properties of all the relevant phenomena associated with the IP shocks: ICME type (MC or EJ), CME properties, solar sources, and the radio emission characteristics.

[9] Based on the IP shocks and their arrival times listed in paper 1, we have identified the SC/SIs events and measured their amplitudes from the *SYM-H* index [*Iyemori*, 1990; *Iyemori and Rao*, 1996] with a time resolution of 1 min obtained from World Data Center, Kyoto, Japan. An SC/SI event is defined as an abrupt increase of the *SYM-H* value with time variation of more than 1.5 nT/min and an amplitude increase of more than 5 nT, as in the work by *Shinbori et al.* [2002, 2003]. For each SC event, the onset time is determined from the H component geomagnetic variation in the rapid sampling records (with the time resolution of 1 m) obtained at Alibag (ABG) Observatory (geographic latitude 18.62°; geographic longitude72.87°; geomagnetic latitude 10.32°) magnetic observatory of Indian Institute of Geomagnetism (IIG), India. Only those SC/SIs events that temporally correspond with the IP shock timings have been selected. The SC events have been taken from the available geomagnetic data yearly bulletins which are published by IIG. The IP shocks and related SC/SI amplitudes in H component and timings have been noted from the ABG. The ABG observatory, away from the influence of equatorial

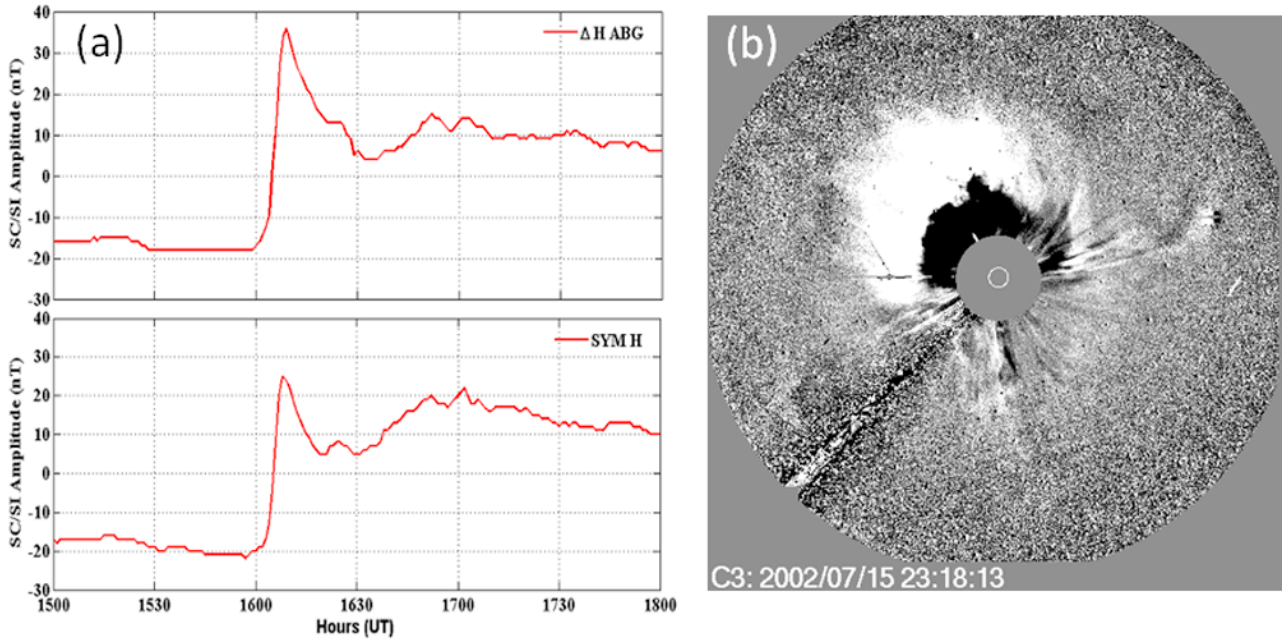

Figure 1. (a) An example of the SC/SI amplitude (top) from the Alibag (ABG) data and (bottom) the *SYM-H* index observed on 17 July 2002 at 16:10 UT, which is followed by the IP shock at 15:50 UT. The SC/SI amplitude in *SYM-H* is 44 nT and in ΔH at ABG is 54 nT. (b) A snapshot of the CME at 23:18 UT observed by the Large Angle and Spectrometric Coronagraph (LASCO) on board SOHO. The bright material in the NE direction is the CME. The fuzzy feature surrounding the CME is the CME-driven shock.

electrojet (EEJ) currents, is one of the prime contributors of geomagnetic field data to World Data Center (WDC), Kyoto, Japan, for calculating the storm time disturbance index (*Dst*). It is found that there is not much difference between the SC/SI amplitudes obtained from *SYM-H* and from ABG H component. The IIG data bulletins consist of complete list of SCs which are followed by geomagnetic storms observed at all Indian magnetic observatories and published every year. Some of the SCs without magnetic storms are not listed in the bulletins. Due to this, we have used both data sets of *SYM-H* and ABG-H components constituting ∼30% and 70%, respectively. In this paper, we use the term SC/SI, because we are considering the both events. Both these data sets provide almost complete list of clear SC/SI events that match well with the IP shocks timings. For 19 IP shocks, the corresponding SC/SI events could not be identified, probably due to the very weak or unclear signatures. However, the above criterion of SC/SI events (*SYM-H* ≥ 5 nT) possibly includes other geomagnetic disturbances such as an abrupt increase of the H component geomagnetic field during the early recovery phase of geomagnetic storms or positive bay phenomena associated with the onset of substorms [*Shinbori et al.*, 2009]. These geomagnetic disturbance events in the *SYM-H* index were excluded after checking the H component geomagnetic field data obtained from several stations in the low-latitude region or a sudden enhancement of solar wind dynamic pressure in the ACE data. Elimination of these unclear events resulted in a set of 203 IP shocks, which we study in this paper. Out of the 203 shocks, 130 were RL and the remaining 73 were RQ. The fraction of RQ shocks (36%) is similar to the one reported in paper 1 (34%).

[10] Figure 1 shows an example of a SC event observed at 16:10 UT on 17 July 2002. The SC/SI amplitude of 44 nT is noted in the *SYM-H* data, while an amplitude of 54 nT in the H component can be found in the ABG data. This SC/SI was observed following the IP shock arrival at 15:50 UT at L1 with a speed of 493 km/s (as listed in paper 1). The IP shock was found to be driven by EJ with a speed of 450 km/s. The source of the IP shock disturbances is a CME at the Sun originating from close to the Sun center (heliographic coordinates N18W01). The CME first appeared in the SOHO coronagraph field of view at 21:30 UT and traveled toward Earth with a speed of 1300 km/s. A snapshot of the CME can be seen in Figure 1b. The small ICME and shock speed at 1 AU suggest that this CME underwent severe deceleration between the Sun and Earth. The CME was associated with a type II radio burst observed by the WAVES experiment onboard the Wind spacecraft, and hence is a RL CME. Details on the CME and the radio burst can be found in paper 1 and in the CME catalog: http://cdaw.gsfc.nasa.gov/CME_list [*Gopalswamy et al.*, 2009b]. The CME was also associated with a large solar energetic particle event [*Gopalswamy et al.*, 2004], which is another indication of the CME-driven shock near the Sun. Figure 2 shows the scatterplot between the CME speed and SC/SI amplitudes for all the events (203) considered in this paper. The SC amplitude ranges from 5 to 128 nT, while the CME speed ranges from ∼100 km/s to more than 3000 km/s. There is a clear indication that faster CMEs produce stronger SC/SI events, although the scatter is relatively large.

3. CMEs Driving Shocks and ICMEs

[11] In this section, we compare the properties of CMEs/ICMEs/IP shocks with those of SC/SI events.

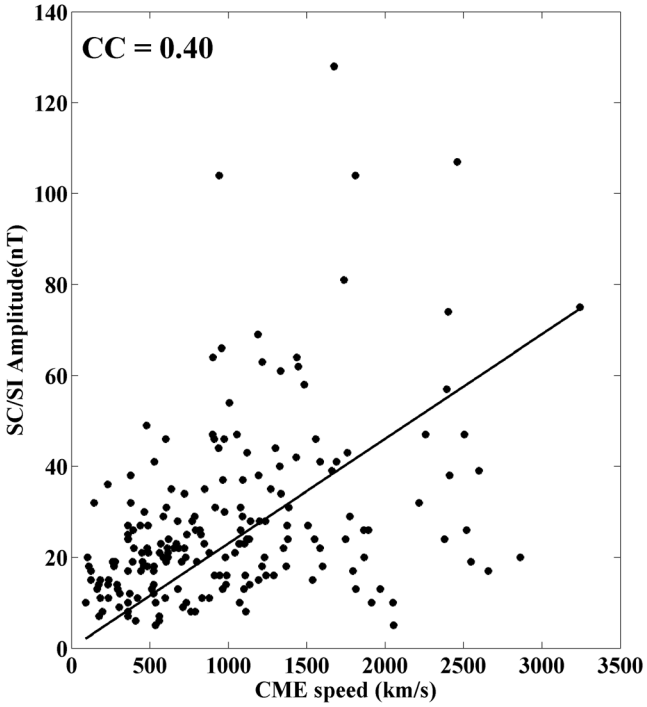

Figure 2. Scatterplot between SC/SI amplitude and CME speed. The correlation coefficient (CC) is 0.40, and SC amplitude ranges from 5 to 128 nT.

Figure 3 shows the distributions of CME, ICME, and IP shock speeds associated with the SC/SI events. The average and median speeds and the standard deviation in speeds are given in Figure 3. The general details on the CME, ICME, and IP shock speeds can be found in Figures 2 and 4 in paper 1 irrespective of their association with SC. The average speed of CMEs is 1015 km/s, which is about a factor 2 higher than the average speed of the general population of CMEs (457 km/s). The average speed of SC-causing CMEs is slightly higher than all shock-driving CMEs (999 km/s) (Figure 4 in paper 1). The high CME average speed indicates that SC/SI-associated CMEs are more energetic than the general CMEs. The average ICME speed is 530 km/s (Figure 3), which is slightly higher than the general RQ ICME speed (446 km/s) and less than the RL ICME speed (572 km/s). (The numbers in parentheses are taken from Table 4 in paper 1.) The average speed of IP shock is 557 km/s which is also higher than the general average RQ IP shock speed (455 km/s) and less than the average RL IP shock speed (608 km/s). This analysis suggests that the RL ICMEs and IP shocks speeds are strong enough to produce higher SC/SI than RQ ICMEs/ IP shocks speeds which are consistent with the studies of paper 1 and with the results of *Gopalswamy et al.* [2008b].

[12] Figure 4 shows the plots of SC/SI amplitude as a function of solar latitude and longitude for all, RL, and RQ shocks with subgroups of MC and EJ. The solar source locations for CMEs given in paper 1 have been used for their associated IP shocks with subgroups of RL and RQ. The average latitudes and longitudes are provided in Tables 1a and 1b. The latitudinal distribution of the SC/SI producing RL and RQ shock sources shows a decline toward limbs with the sharp cutoff around $\pm 30^\circ$ latitude for all events. Most of shocks are observed between the northern and southern active regions which are much more pronounced for RL shocks than RQ shocks. The average latitude for RL shocks is less than for RQ, which suggests that the shock-driving CMEs originate in the active region belt as these regions have higher magnetic field, thus resulting in more energetic CMEs. The average latitude for MC-associated RL shocks is higher than that of the EJ-associated RL shocks. In the case of solar longitude, it is found that the longitude distribution spreads over entire longitude belt for RL shocks than RQ shocks. The average value of CME longitude for MC-associated RL shocks is less than that for EJ-associated RL shocks. The latitudinal distribution combined with longitudinal distribution shows that the source locations are different for RL and RQ shocks with RL shocks distributed more widely along longitudes. The average longitude of the distribution is higher for RL shocks than for RQ shocks.

[13] Most of the shocks are followed by the ICMEs, which are either MCs or non cloud EJ. There were 109 EJ and 56 MC events in the list of paper 1. Figure 5 shows the scatterplots of SC/SI amplitude against the speeds of ICMEs (MC and EJ shown separately) and IP shocks. Table 2 shows the comparison of the average ICME and shock speeds. The SC/SI

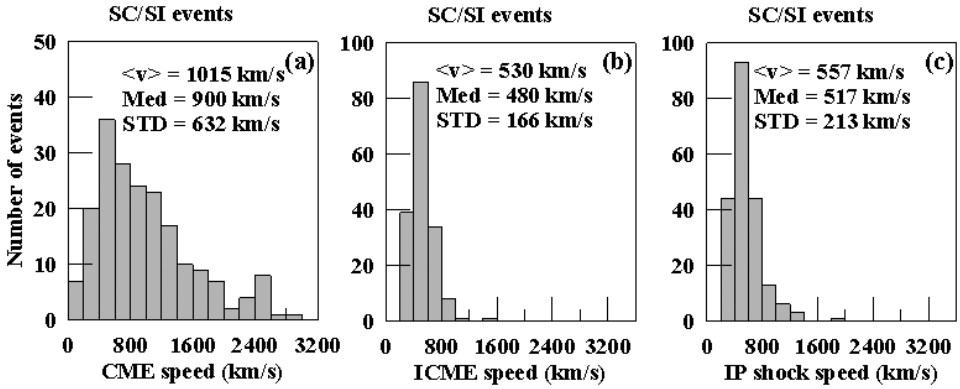

Figure 3. The distribution of (a) CME, (b) ICME, and (c) IP shock speeds for SC/SI producing events. The bin size is 200 km/s. The average mean ($\langle V \rangle$), median and standard deviation (STD) of speeds in each case are given.

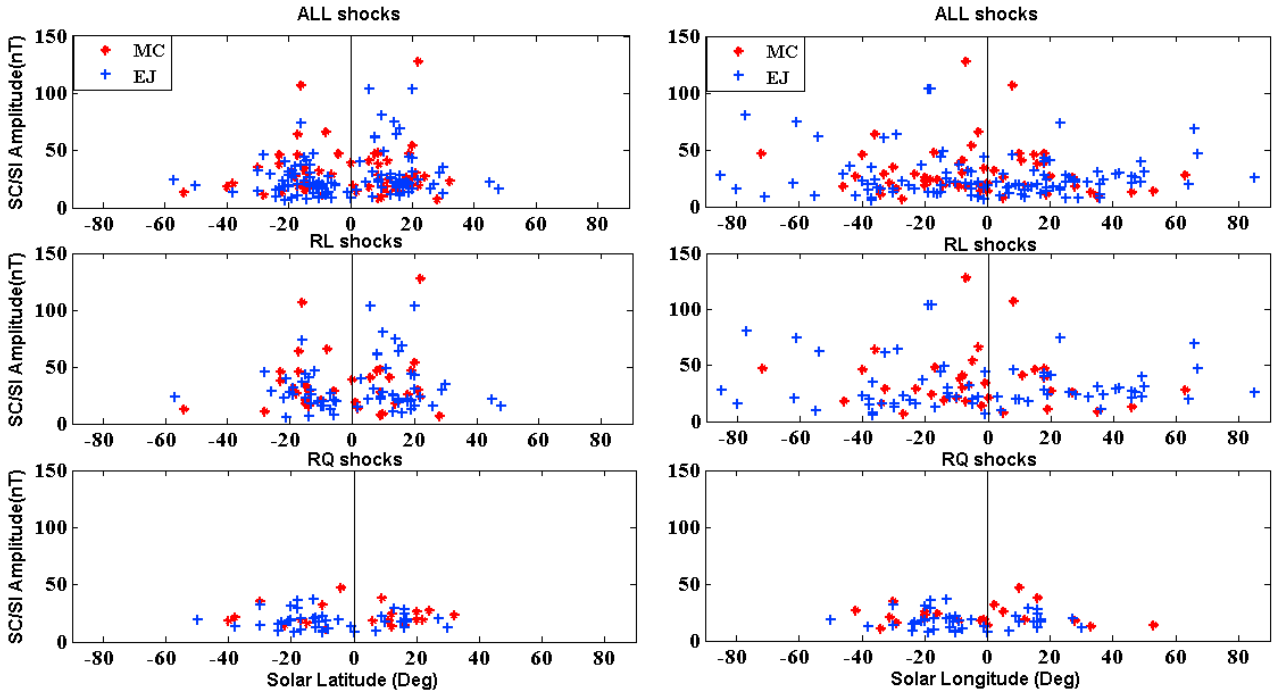

Figure 4. SC/SI amplitude variation with solar latitude and longitude for all, RL and RQ shocks. The ICMES are divided in MCs (red pluses) and EJs (blue pluses) are shown. The average values of all, RL and RQ shocks with separation of MCs and EJs are given in Tables 1a and 1b.

amplitudes for IP shocks are given in Table 2. The shock speeds are generally higher for the MCs and the corresponding SC amplitudes are also higher. The difference in speeds is attributed to the fact that the MC-associated shocks are measured at their noses, hence they have higher the speed, whereas EJ-associated shocks are measured between their nose and flanks, so they have lesser speed and hence give the difference in the SC/SI amplitudes. The CME speeds associated with MC and EJ events are also shown in Table 2. The CME speed near the Sun is generally opposite to that seen in ICMEs. The CME speeds are much higher near the Sun than those of the IP counterparts because CMEs undergo deceleration in the IP medium due to the interaction with the solar wind [see, e.g., *Gopalswamy et al.*, 2000]. The higher speeds of EJ CMEs compared to the MC CMEs can be attributed to the fact that the latter are subject to more projection effects due to their origin close to the disk center. This explanation is based on the commonly accepted view that all ICMEs are flux ropes and the appearance as EJ or MC is an observational effect. This has been shown to be true in the zeroth-order approximation [*Gopalswamy et al.*, 2006]. There can be a significant deviation from the approximation. One can see EJ sources and even driverless shock sources from the disk center. The driverless shocks from the disk center have been explained by nearby coronal holes [*Gopalswamy et al.*, 2009a] such that disk center CMEs behave like limb CMEs. There may be many reasons as to why disk center CMEs become EJs rather than MCs nonradial eruption, CME deflection and other propagation effects. Table 2 summarizes the resulting correlation coefficients (CC). All correlations are positive with CC $\geq$ 0.40. The MC speeds and their shocks show better correlations with the SC amplitude (0.64 and 0.68, respectively). The best correlation is between speeds of MC-driven shocks and the SC amplitude. These results are consistent with the fact that the associated CMEs originate close to the disk center of the Sun and hence represent a direct impact on the magnetosphere. Since the SC is caused by the shock rather than the ICME, the MC-driven shocks are the most effective in producing higher SC/SI amplitudes. The EJ–CMEs originate from intermediate central meridian region on the Sun and hence represent slightly reduced impact on the magnetosphere, thus contributing to the decorrelation between shock speed and SC amplitude. Also, a large number of SC/SIs is

Table 1a. The Average Values of Latitude and Longitude for All, RL, RQ Shocks[a]

	Latitude (°N)	Latitude (°S)	Longitude (°E)	Longitude (°W)
All shocks	15	18	23	23.5
RL shocks	14.5	17	28	25
RQ shocks	16	19.5	17	22

[a]From Figure 4.

Table 1b. The Average Values of Latitude and Longitude for MC and EJ Type[a]

	Latitude (°N)		Latitude (°S)		Longitude (°E)		Longitude (°W)	
	MC	EJ	MC	EJ	MC	EJ	MC	EJ
All shocks	15	15.5	19.5	17	19.5	26	20	27
RL shocks	13	16	18.5	16	22.5	34	19.5	30
RQ shocks	17	15	20.5	18.5	16.5	17.5	21	23.5

[a]From Figure 4.

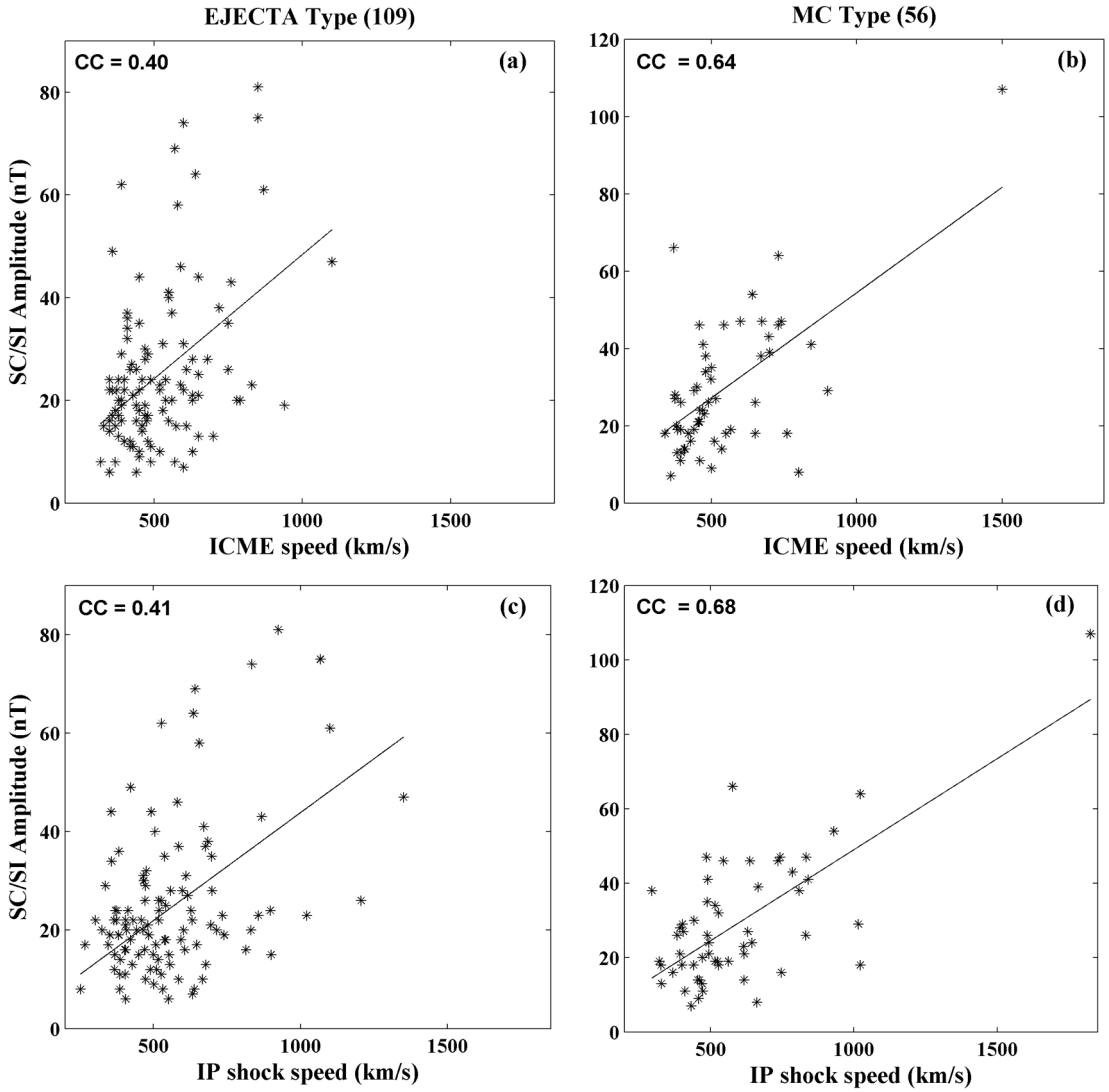

Figure 5. Scatterplot showing the ICME/IP shock speed with SC/SI amplitude for MCs (56) and EJs (109). The correlation coefficients (CC) are given. The average SC amplitude and IP shock speed are given in Table 2.

produced by the ICME and IP shocks with lower speeds on the average.

4. Radio-Loud and Radio-Quiet Shocks

[14] We have divided the SC/SI events into two subgroups associated with RL and RQ shocks. Figure 6 shows the number of SC/SI produced events in each category of CME, ICME, and IP shock for RL and RQ shocks (Figure 6a). It is obvious from Figure 6b that RL shock-associated events occur more frequently than the RQ shock-associated events. The comparison of the average SC/SI amplitudes for RL and RQ shocks in all CME, ICME, IP Shock categories shown in Figure 6b reveals that RL shocks are most effective in causing SC/SI events. We divided the SC/SI events into two subgroups associated with RL and RQ shocks. Figure 7 shows the SC/SI amplitude distributions for all (RL+RQ) shocks, RL shocks, and RQ shocks. It can be seen from Figure 6 that SC/SI amplitudes associated with RL shocks are higher (average ~32 nT) than those associated with RQ shocks (average ~19 nT). The average SC/SI amplitude for RL shocks is almost a factor of 1.6 higher than that for RQ

Table 2. Comparison of Shock Speeds and Amplitudes for EJ and MC[a]

	EJ	MC
	Average SC/SI amplitude (nT)	
IP Shock	22.34	29.01
	Average Speed(km/s)	
ICME	488.07	520.92
IP Shock	519.77	589.87
CME	1119	1058
	Correlation Coefficients	
ICME	0.40	0.64
IP Shock	0.41	0.68

[a]From Figure 5.

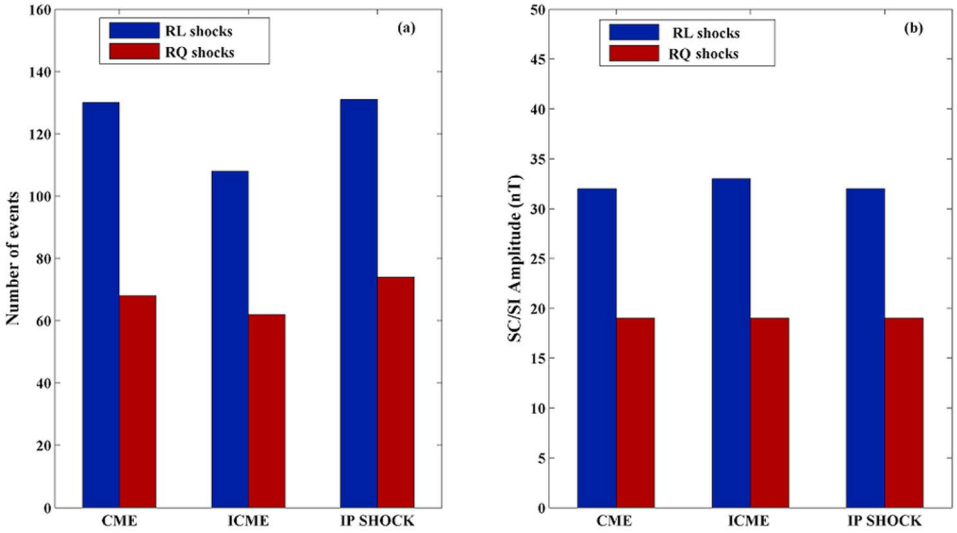

Figure 6. (a) The distribution of CME/ICME/IP shocks for RL and RQ events. (b) The average SC/SI amplitude for RL and RQ shocks with the distribution of CME/ICME/IP shock.

shocks. The higher average SC/SI amplitude observed for RL shocks suggests that the RL shocks are more energetic than the RQ shocks and hence are more effective in producing SCs.

[15] The correlation of SC/SI amplitude with CME and IP shock speeds for RL and RQ shocks is shown in Figure 8. We have not considered ICMEs because there is not much difference between the average speeds of ICMEs and IP shocks. The MCs and EJ are shown separately for all, RL and RQ shocks. Table 3a shows the average SC/SI amplitude and average CME speed and IP shock speed for RL and RQ subgroups. Table 3b gives the comparison of the correlation coefficients (from Figure 8) showing that the correlation is better for RL shocks in the category of MCs than EJs. The poor correlation coefficients obtained for the RQ shocks in three categories (Figures 8e and 8f) are due to the difference in locations where shock speed is measured and the shock evolution between the Sun and Earth. MCs head directly toward Earth, so the shock measurement is made at the nose where the speed is the maximum. For EJ, the CME heads not directly at Earth, so the shock speed is measured slightly away from the nose hence the speed may be smaller. This explains the difference between MC and EJ correlations because of the speed difference. As for the difference between RL and RQ shocks, the associated CMEs have different kinematic evolution. The RL CMEs start with very high speed near the Sun and slowly decelerate. On the other hand, the RQ CMEs start out very slowly and reach higher speeds far into the IP medium, where they start driving a shock. The CME speed for the RL shocks is thus better correlated with the SC/SI amplitude. The RQ shocks are generally slower because the associated CMEs barely become super-Alfvenic (they do not produce a type II burst). It can be noted from Table 3a that average speed and amplitude for RL shocks are higher than for RQ shocks which explains that the RL shocks are more effective in generating SC/SIs than RQ shocks.

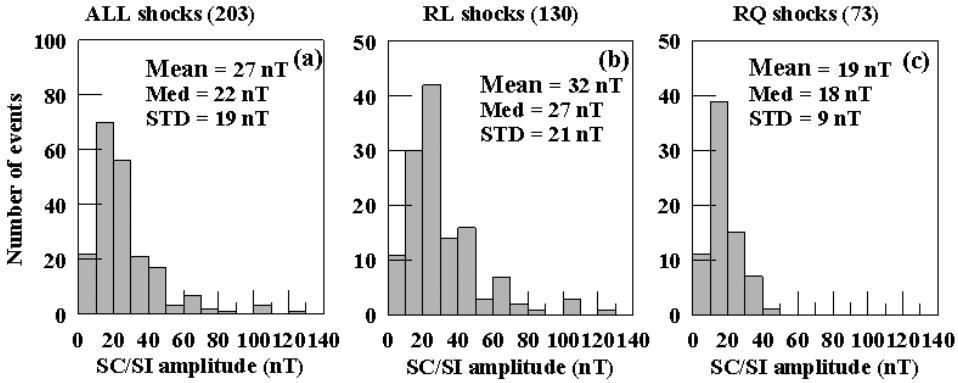

Figure 7. The distribution of SC/SI amplitude for (a) all, (b) RL and (c) RQ events. The average mean (⟨V⟩), median, and standard deviation (STD) for each case are given. The bin size is 20 nT.

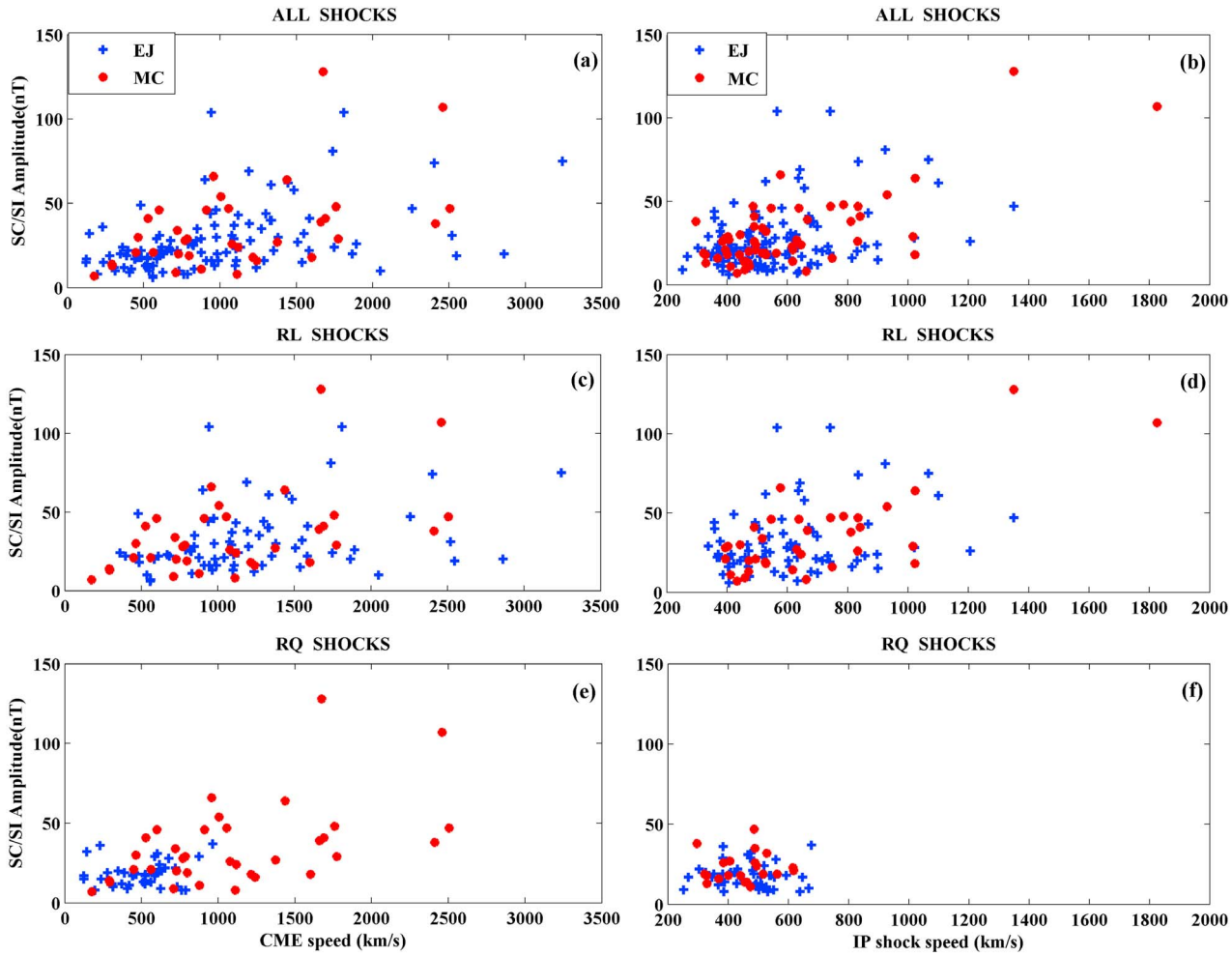

Figure 8. The scatterplot for CME/IP shock speed with SC/SI amplitude for all, RL and RQ shocks for MCs (red pluses) and EJs (blue pluses). The average SC amplitude and speed are given in Table 3a. The correlation coefficients (CC) are given in the Table 3b for all, MCs and EJs with RL and RQ shocks.

[16] In order to further quantify the strength of the shocks associated with SC/SI amplitude, we have compared the Alfvenic Mach numbers (M_A) of the IP shocks from paper 1 with the associated SC/SI amplitudes. In Figure 9, we have plotted the SC/SI amplitude as a function of the M_A for all, RL, and RQ shocks. The SC/SI amplitudes for RQ shocks are generally low compared to those of RL shocks and the M_A have a similar distribution. The correlation coefficient between SC/SI amplitude and M_A is higher for RL shocks compared to RQ shocks. The average M_A (2.6) for RQ shocks is less than that for RL shocks (3.4) by ~31%. This difference is also consistent with the SC/SI amplitudes for RL shocks. The difference in M_A reflects the difference in CME speed for RQ and RL shocks and also confirms that RQ shocks are weaker.

5. Discussion and Conclusion

[17] Using the list of CME-driven shocks observed at 1 AU and their association with type II radio bursts compiled

Table 3a. CME and IP Shocks for RL and RQ[a]

	RL	RQ
	Average SC/SI Amplitude (nT)	
CME	31.81	18.74
IP shock	31.67	18.54
	Average Speeds (km/s)	
CME	1259	476
IP shock	617	457

[a]From Figure 8.

Table 3b. Correlation Coefficients for All Shocks, RL Shocks and RQ Shocks With Separation of ICME Types, MC and EJ[a]

	CME		IP Shock	
	MC	EJ	MC	EJ
All shocks	0.55	0.45	0.73	0.36
RL shocks	0.50	0.31	0.74	0.29
RQ shocks	0.50	0.18	0.07	−0.02

[a]From Figure 8.

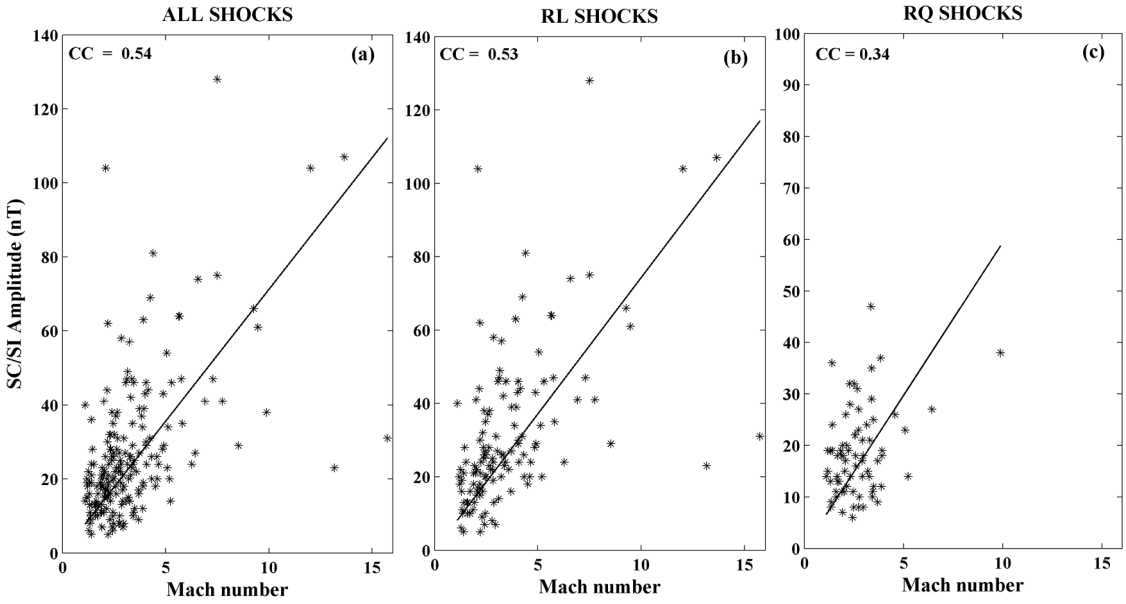

Figure 9. Scatterplot of Mach number with SC/SI amplitude for all, RL and RQ shocks. The correlation coefficients (CC) are given.

in paper 1 we have analyzed the corresponding SC/SI events. We subdivided the IP shocks into RL and RQ shocks and found that RL shocks are generally more effective in producing SC events. We have further investigated the SC/SI amplitude variation with ICME (associated with MC and EJ) speeds and shock M_A. The shocks associated with MC type ICMEs are more effective in causing SC events. As shown in paper 1, CMEs associated with RQ shocks have lower energy compared to the RL shocks. These two shock populations differ in many other aspects such as speed and acceleration. In general, all the parameters of RQ CMEs show lower CME energy, resulting in weaker shocks and hence weaker SCs. However, the average speed of CMEs associated with RQ shocks slightly higher than that of the general population of CMEs. The importance of identifying RL CMEs from near the disk center is thus clearly of forecast value because such CMEs result in strong SC events.

[18] *Cho et al.* [2010] found a better correlation (CC = 0.67) between CME speed and the SC/SI amplitude caused by IP shocks for fast CMEs (V_{CME} > 1000 km/s) using only 26 type II burst IP shocks. But we have considered 203 IP shocks (including RL and RQ shocks) and correlation coefficient is 0.55 between CME speed and SC/SI amplitude (Figure 8). We further isolate RL and RQ shocks which are associated with MCs and EJs, the correlation (0.50) is better for RL and RQ shocks associated with MCs than EJs (Table 3b). This correlation is lower than the correlation obtained by *Cho et al.* [2010] due to analysis of large number IP shocks. The average SC/SI amplitude and CME speed are higher for RL shocks than RQ shocks.

[19] Paper 1 showed that out of a total 180 shocks associated with ICMEs, 32% of shocks were driven by MCs, 68% were driven by noncloud EJ. Also 42 out of 222 IP shocks (19%) were driverless. The present study shows better correlation for SC/SI amplitude with MC-associated shocks than EJ-associated shocks. Though the MC-associated shocks have lower CME speed than EJ-associated shocks but MCs have the strong effect in producing SC/SIs due to their difference in solar source distributions. Also, the better correlation between SC/SI amplitude and MC speed is due to the difference in the way the speeds were measured. The MC-associated shocks are measured at their noses where they have highest speed (625 km/s) and the EJ-associated shocks are measured between their nose and flanks where they have intermediate speed (549 km/s). Thus, MCs are more effective in producing higher SC/SI amplitudes.

[20] Our analysis clearly shows that RQ shocks produce smaller SC/SI amplitude than the RL shocks do. According to paper 1, a positive acceleration is shown by most of the CMEs associated with RQ shocks and a negative acceleration of the CMEs associated with RL shocks. This means that the RQ shocks are formed generally at large distances from the Sun ($\geq$10 R_s) where the driving CMEs become super-Alfvenic. Thus, RQ shocks are the weakest, followed by shocks producing the type II radio bursts, and the shocks producing radio emission at higher frequencies. The primary characteristic that distinguishes between RQ and RL shocks seems to be the kinetic energy of the CME drivers. The low M_A for RQ shocks is consistent with the low-energy drivers associated with them whereas RL shocks have large average ($\sim$3.4) M_A. One of the practical implications of these results is that when a CME near the Sun does not produce a type II radio burst, it is unlikely that this CME will result in a large SC event. Such a conclusion was also derived from the occurrence of another 1 AU event, namely, energetic storm particle (ESP) events caused by IP shocks by *Mäkelä et al.* [2011]. They found that RL shocks associated with the MC events produce the largest ESP events. It must be noted that the same shock produces SC and ESP event at 1 AU by different physical mechanisms.

[21] Paper 1 reported a significant number of (42 out of 222 or 19%) driverless shocks, which means that the shocks

may not be followed by discernible driver. In this work, there are 38 driverless shocks which are associated with SC/SI events (38 out of 203 or 18.7%) with 25 RL and 13 RQ shocks. The average SC amplitude is 25 nT and 15 nT for RL and RQ shocks (driverless), respectively. The average SC/SI amplitude for driverless RL shocks is higher than the shocks which are associated with EJ and is lower than for the shocks with MCs.

[22] The distribution of solar sources over the solar surface shows that the RL shocks are spread over the entire longitude belt (Figure 4) than RQ shocks of which the source region is mainly confined to $\pm 30^{\circ}$. So, the RQ and RL source distributions reflect the width of the shock front ahead of a propagating CME. *Gopalswamy et al.* [2010] reported that the RL CMEs and the associated shocks are faster, i.e., are more energetic, than the RQ CMEs and shocks. Faster CMEs are generally wider, therefore the wider RL shocks with a larger longitudinal separation between the solar source and the observer can still be detected at 1 AU. In a study of CME widths, *Michalek et al.* [2007] reported that RL CMEs are almost two times wider than RQ CMEs. The source distribution of RQ and RL shocks considerably different from that of RQ and RL fast and wide CMEs [*Gopalswamy et al.*, 2008a]. They found that the sources of RQ CMEs are located near the limbs whereas for RL CMEs occur in central west regions of the solar disk. There exists a similar variation in SC/SI amplitudes with respect to the solar latitude and longitude. The difference in the source distribution is due to the selection effect because we consider only CMEs that produce a shock signature at 1 AU.

[23] The main findings of the present study are summarized as follows.

[24] About 91% of shocks produced clear SC/SI events. The average speed of SC/SI-associated CME is 1015 km/s, which is almost a factor of 2 higher than that of the general CME population. MC-associated shock speeds are better correlated with SC/SI amplitudes as compared to the EJ shocks. Also SC/SI amplitudes are higher for MCs than EJ-associated shocks. The average SC/SI amplitudes for RL and RQ shocks are 32 and 19 nT, respectively. RL shocks are more effective in producing SC/SI events than the RQ shocks. The average M_A is higher for RL shocks than for RQ shocks. The SC/SI amplitudes and M_A of the shocks are better correlated with RL shocks than with the RQ shocks. Thus, if we observe a RL CME near the Sun originating close to the disk center, it is highly likely that the shock produces a large SC/SI event at Earth. There is a significant difference in the latitudinal and longitudinal distribution for RL and RQ shocks associated with SC/SI amplitudes. RL shocks are spread over more of the longitude belt than RQ shocks. RQ shock source region is confined to $\pm 30^{\circ}$.

[25] **Acknowledgments.** We thank the World Data Center for Geomagnetism, Kyoto, for *SYM-H* data. Part of the first author's work was supported by the Nagoya University, Nagoya, Japan. The work of N. Gopalswamy was supported by NASA's Living with a Star (LWS) program.

[26] Philippa Browning thanks the reviewers for their assistance in evaluating this paper.

References

Araki, T. (1977), Global structure of geomagnetic sudden commencements, *Planet. Space Sci.*, *25*, 373–384, doi:10.1016/0032-0633(77)90053-8.

Chao, J. K., and R. P. Lepping (1974), A correlative study of SSC's interplanetary shocks, and solar activity, *J. Geophys. Res.*, *79*, 1799–1807, doi:10.1029/JA079i013p01799.

Chi, P. J., D.-H. Lee, and C. T. Russell (2006), Tamao travel time of sudden impulses and its relationship to ionospheric convection vortices, *J. Geophys. Res.*, *111*, A08205, doi:10.1029/2005JA011578.

Cho, K. S., S. C. Bong, Y. J. Moon, M. Dryer, S. E. Lee, and K. H. Kim (2010), An empirical relationship between coronal mass ejection initial speed and solar wind dynamic pressure, *J. Geophys. Res.*, *115*, A10111, doi:10.1029/2009JA015139.

Gonzalez, W. D., J. Joselyn, Y. Kamide, H. Kroehl, G. Rostoker, B. Tsurutani, and V. Vasyliunas (1994), What is a magnetic storm?, *J. Geophys. Res.*, *99*, 5771–5792, doi:10.1029/93JA02867.

Gopalswamy, N. (2008), Type II radio emission and solar energetic particle events, in *Particle Acceleration and Transport in the Heliosphere and Beyond*, edited by G. Li et al., *AIP Conf. Ser.*, *1039*, 196–202.

Gopalswamy, N. (2009), Coronal mass ejections and space weather, in *Climate and Weather of the Sun-Earth System (CAWSES), Selected Papers From the Kyoto Symposium 2007*, edited by T. Tusuda et al., pp. 77–120, TERRAPUB, Tokyo.

Gopalswamy, N., A. Lara, R. P. Lepping, M. L. Kaiser, D. Berdichevsky, and O. C. St. Cyr (2000), Interplanetary acceleration of coronal mass ejections, *Geophys. Res. Lett.*, *27*, 145–148, doi:10.1029/1999GL003639.

Gopalswamy, N., S. Yashiro, S. Krucker, G. Stenborg, and R. A. Howard (2004), Intensity variation of large solar energetic particle events associated with coronal mass ejections, *J. Geophys. Res.*, *109*, A12105, doi:10.1029/2004JA010602.

Gopalswamy, N., E. Aguilar-Rodriguez, S. Yashiro, S. Nunes, M. L. Kaiser, and R. A. Howard (2005), Type II radio bursts and energetic solar eruptions, *J. Geophys. Res.*, *110*, A12S07, doi:10.1029/2005JA011158.

Gopalswamy, N., Z. Mikić, D. Maia, D. Alexander, H. Cremades, P. Kaufmann, D. Tripathi, and Y.-M. Wang (2006), The pre-CME Sun, *Space Sci. Rev.*, *123*, 303–339, doi:10.1007/s11214-006-9020-2.

Gopalswamy, N., S. Yashiro, S. Akiyama, P. Mäkelä, H. Xie, M. L. Kaiser, R. A. Howard, and J. L. Bougeret (2008a), Coronal mass ejections, type II radio bursts, and solar energetic particle events in the SOHO era, *Ann. Geophys.*, *26*, 3033–3047, doi:10.5194/angeo-26-3033-2008.

Gopalswamy, N., S. Yashiro, H. Xie, S. Akiyama, S. E. Aguilar-Rodriguez, M. L. Kaiser, R. A. Howard, and J. L. Bougeret (2008b), Radio-quiet fast and wide coronal mass ejections, *Astrophys. J.*, *674*, 560–569, doi:10.1086/524765.

Gopalswamy, N., P. Mäkelä, H. Xie, S. Akiyama, and S. Yashiro (2009a), CME interaction with coronal holes and their interplanetary consequences, *J. Geophys. Res.*, *114*, A00A22, doi:10.1029/2008JA013686.

Gopalswamy, N., S. Yashiro, G. Michalek, G. Sternborg, A. Vourlidas, S. Freeland, and R. Howard (2009b), The SOHO/LASCO CME Catalog, *Earth Moon Planets*, *104*, 295–313, doi:10.1007/s11038-008-9282-7.

Gopalswamy, N., H. Xie, P. Mäkelä, S. Akiyama, S. Yashiro, M. L. Kaiser, R. A. Howard, and J. L. Bougeret (2010), Interplanetary shocks lacking type II radio bursts, *Astrophys. J.*, *710*, 1111, doi:10.1088/0004-637X/710/2/1111.

Iyemori, T. (1990), Storm-time magnetospheric currents inferred from mid-latitude geomagnetic field variations, *J. Geomagn. Geoelectr.*, *42*, 1249–1265, doi:10.5636/jgg.42.1249.

Iyemori, T., and D. R. K. Rao (1996), Decay of the *Dst* field of geomagnetic disturbance after substorm onset and its implication to storm-substorm relation, *Ann. Geophys.*, *14*, 608–618, doi:10.1007/s00585-996-0608-3.

Mäkelä, P., N. Gopalswamy, S. Akiyama, H. Xie, and S. Yashiro (2011), Energetic storm particle events in coronal mass ejection–driven shocks, *J. Geophys. Res.*, *116*, A08101, doi:10.1029/2011JA016683.

Michalek, G., N. Gopalswamy, and H. Xie (2007), Width of radio-loud and radio-quiet CMEs, *Sol. Phys.*, *246*, 409–414, doi:10.1007/s11207-007-9062-y.

Shinbori, A., T. Ono, and H. Oya (2002), SC-triggered plasma waves observed by the Akebono satellite in the polar regions and inside the plasmasphere, *Adv. Polar Upper Atmos. Res.*, *16*, 126–135.

Shinbori, A., T. Ono, M. Iizima, A. Kumamoto, and H. Oya (2003), Sudden commencements related plasma waves observed by the Akebono satellite in the polar region and inside the plasmasphere region, *J. Geophys. Res.*, *108*(A12), 1457, doi:10.1029/2003JA009964.

Shinbori, Y. T., T. Kikuchi, T. Araki, and S. Watari (2009), Magnetic latitude and local time dependence of the amplitude of geomagnetic sudden commencements, *J. Geophys. Res.*, *114*, A04217, doi:10.1029/2008JA013871.

Smith, E. J., B. T. Tsurutani, J. A. Slvain, D. E. Jones, G. L. Siscoe, and D. A. Mendis (1986), International Cometary Explorer encounter with Giacobini-Zinner: Magnetic field observations, *Science*, *232*, 382–385, doi:10.1126/science.232.4748.382.

Takeuchi, T., C. T. Russell, and T. Araki (2002), Effect of the orientation of interplanetary shock on the geomagnetic sudden commencement, *J. Geophys. Res.*, *107*(A12), 1423, doi:10.1029/2002JA009597.

Tsurutani, B. T., W. D. Gonzalez, F. Tang, S. I. Akasofu, and E. J. Smith (1988), Origin of interplanetary southward magnetic fields responsible for major magnetic storms near solar maximum (1978–1979), *J. Geophys. Res.*, *93*, 8519–8531, doi:10.1029/JA093iA08p08519.

Wang, C., C. X. Li, Z. H. Huang, and J. D. Richardson (2006), Effect of interplanetary shock strengths and orientations on storm sudden commencement rise times, *Geophys. Res. Lett.*, *33*, L14104, doi:10.1029/2006GL025966.

Wang, C., J. B. Liu, H. Li, Z. H. Huang, J. D. Richardson, and J. R. Kan (2009), Geospace magnetic field responses to interplanetary shocks, *J. Geophys. Res.*, *114*, A05211, doi:10.1029/2008JA013794.

Wang, C., H. Li, J. D. Richardson, and J. R. Kan (2010), Interplanetary shock characteristics and associated geosynchronous magnetic field variations estimated from sudden impulses observed on the ground, *J. Geophys. Res.*, *115*, A09215, doi:10.1029/2009JA014833.

Wilken, B., C. K. Goertz, D. N. Baker, P. R. Higbie, and T. A. Fritz (1982), The SSC on July 29, 1977 and its propagation within the magnetosphere, *J. Geophys. Res.*, *87*(A8), 5901–5910, doi:10.1029/JA087iA08p05901.

N. Gopalswamy, Heliophysics Division, NASA Goddard Space Flight Center, Bldg. 21, Rm. 170, Code 671, Greenbelt, MD 20771, USA.

T. Kikuchi, Solar-Terrestrial Environment Laboratory, Nagoya University, Nagoya 464-8601, Aichi, Japan.

S. Kumar, School of Engineering and Physics, University of the South Pacific, Private Mail Bag, Laucala Campus, Suva, Fiji.

A. K. Maurya, R. Selvakumaran, and B. Veenadhari, Department of Science and Technology, Indian Institute of Geomagnetism, Kalamboli Highway, New Panvel, Navi Mumbai, Maharastra 410 210, India. (veenaiig@gmail.com)

R. Singh, Dr. K. S. Krishnan Geophysical Research Laboratory, Indian Institute of Geomagnetism, Jhunsi, Allahabad, Uttar Pradesh 221505, India.